ISSN 1674-1056
http://cpb.iphy.ac.cn
http://iopscience.iop.org/cpb
中国物理 B
Chinese Physics
中国物理
Chinese Physics B

Dissipative generation for steady-state entanglement of two transmons in circuit QED

Shuang He(何爽), Dan Liu(刘丹), Ming-Hao Li(李明浩)

Citation: Chin. Phys. B . 2019, 28(8): 080303 . **doi:** 10.1088/1674-1056/28/8/080303
Journal homepage: http://cpb.iphy.ac.cn; http://iopscience.iop.org/cpb

What follows is a list of articles you may be interested in

Tetrapartite entanglement measures of W-class in noninertial frames

Ariadna J. Torres-Arenas, Edgar O. López-Zúñiga, J. Antonio Saldaña-Herrera, Qian Dong, Guo-Hua Sun, Shi-Hai Dong
Chin. Phys. B . 2019, 28(7): 070301 . **doi:** 10.1088/1674-1056/28/7/070301

Entropy squeezing for three-level atom interacting with a single-mode field

Fei-Fan Liu(刘非凡), Mao-Fa Fang(方卯发), Xiong Xu(许雄)
Chin. Phys. B . 2019, 28(6): 060304 . **doi:** 10.1088/1674-1056/28/6/060304

Steady-state entanglement and heat current of two coupled qubits in two baths without rotating wave approximation

Mei-Jiao Wang(王美姣), Yun-Jie Xia(夏云杰)
Chin. Phys. B . 2019, 28(6): 060303 . **doi:** 10.1088/1674-1056/28/6/060303

Quantifying quantum non-Markovianity via max-relative entropy

Yu Luo(罗宇), Yongming Li(李永明)
Chin. Phys. B . 2019, 28(4): 040301 . **doi:** 10.1088/1674-1056/28/4/040301

Engineering steady-state entanglement for two atoms held in separate cavities through laser cooling

Shen Li-Tuo, Chen Rong-Xin, Wu Huai-Zhi, Yang Zhen-Biao
Chin. Phys. B . 2014, 23(4): 040303 . **doi:** 10.1088/1674-1056/23/4/040303

Dissipative generation for steady-state entanglement of two transmons in circuit QED

Shuang He(何爽), Dan Liu(刘丹), and Ming-Hao Li(李明浩)†

Department of Nuclear Medicine, Yanbian University Hospital, Yanji 133000, *China*

(Received 1 April 2019; revised manuscript received 20 May 2019; published online 25 July 2019)

We present a dissipative scheme to generate an entangled steady-state between two superconducting transmon qutrits separately embedded in two coupled transmission line resonators in a circuit quantum electrodynamics (QED) setup. In our scheme, the resonant qutrit-resonator interaction and photon hopping between resonators jointly induce asymmetric energy gaps in the dressed state subspaces. The coherent driving fields induce the specific dressed state transition and the dissipative processes lead to the gradual accumulation in the population of target state, combination of both drives the system into a steady-state entanglement. Numerical simulation shows that the maximally entangled state can be produced with high fidelity and strong robustness against the cavity decay and qutrit decay, and no requirements for accurate time control. The scheme is achievable with the current experimental technologies.

Keywords: steady-state entanglement, dissipation, dressed state

PACS: 03.67.–a, 03.67.Bg, 32.80.Ee **DOI:** 10.1088/1674-1056/28/8/080303

1. Introduction

In the past decades, quantum entanglement[1,2] as a peculiar nonclassical effect of physical system and an indispensable resource of quantum information has been deeply studied and great progress has been made both theoretically[3] and experimentally,[4] thus greatly promotes the development of quantum computing and quantum communication. The ultimate goal of quantum information is to achieve large scale quantum computing and quantum communication. In this sense, the challenges faced by the field of quantum information in the course of development mainly come from two aspects, one is the maintenance and storage for quantum entanglement, the other is the scalability of the physical system. It is widely convinced that dissipation induced by the environment is the main obstacle in preparing and storing entanglement, for the reason that dissipation may inevitably degrade the coherence of the quantum system. From this perspective it is a negative factor for quantum information processing (QIP) and should be avoided as much as possible. However, recent theories and experiments show an interesting fact that the dissipation can be used as a positive resource for quantum computation and entanglement generation,[5–8] so that an alternative approach for engineering dissipation to generate entanglement has emerged. Many dissipation-assisted entanglement schemes have been proposed with cavity quantum electrodynamics (QED),[9–24] atomic ensembles,[25–27] ion traps,[28–30] plasmonic systems,[31–33] and optical lattices.[34,35] The relevant experimental demonstrations are also have been achieved in atomic ensembles[36] and ion traps.[30] Different from the unitary evolution schemes, these schemes use dissipation as a positive resource in the preparation process, and have the advantages in robustness against decoherence and parameter fluctuations and dose not require a specifical initial state or precise evolution time.[28]

On the other hand, circuit QED can produce an extremely strong interaction between the superconducting qubits and the microwave photons in a transmission line resonator, which is beneficial to quantum system to resist the environmental dissipation and parameter fluctuations.[37] In view of its high integratability, high tunability, and addressability for individual resonators, the circuit QED has been widely regarded as the most promising architectures for QIP.[38–41] It is essential for large scale quantum computation to engineer entanglement in coupled cavity networks, from this perspective, it would be of great importance to prepare entanglement among superconducting qubits in separated resonators. In this paper, based on the circuit QED architecture, we design an alternative scheme to prepare the entangled steady-state of two superconducting transmons separately interact with two transmission line resonators in a coupled circuit QED dimer.[42,43] The resonant transmon-resonator interaction and the photons hopping between two resonators lead to a dressed state subspace of the qutrits with different excitation numbers of photon modes. By employing two specified microwave fields to resonantly drive the system to the well-defined state in dressed state subspace and resorting to the dissipations of photon leakage and qutrit decay, a steady entanglement between two transmons can be obtained. Numerical simulations show that the entangled steady-state can be achieved with high fidelity with current experimental parameters. The scheme is independent of the initial state and robust against parameter fluctuations.

The remainder of the paper is organized as follows. In the Section 2, we describe the interaction system and the dressed state subspace by calculation. In Section 3, the steady-state

†Corresponding author. E-mail: mhli27@sina.com

© 2019 Chinese Physical Society and IOP Publishing Ltd

entanglement of two transmons is obtained by engineering the dissipative dynamics of the system with microwave pulses. In Section 4, the fidelity of the target steady-state and Clauser–Horne–Shimony–Holt (CHSH) correlation are simulated numerically with the current available experimental parameters, by which the feasibility of the present scheme is demonstrated. A conclusion appears in Section 5.

2. The interaction system and the dressed state subspace

The system under consideration is depicted in Fig. 1. It consists of two transmission line microwave resonators coupled through hopping of microwave photons with a hopping rate J that is controllable and could be determined by a coupling capacitance of the resonators. Each resonator can be modeled as a single harmonic oscillator mode of frequency ω_a, and contains a single Λ-type superconducting qutrit which possesses two ground states $|g\rangle$ and $|f\rangle$ and one excited state $|e\rangle$ with the corresponding energies ω_g, ω_f, and ω_e, respectively. The qutrit transition $|f\rangle \leftrightarrow |e\rangle$ is resonantly coupled to the resonator with the coupling constant g, and the transitions $|g\rangle \leftrightarrow |e\rangle$ and $|g\rangle \leftrightarrow |f\rangle$ are driven by two microwave fields with Rabi frequencies Ω_1 and Ω_2, respectively. Then the total Hamiltonian of the system can be written as

$$H = H_{\rm NM} + H_1 + H_2, \tag{1}$$

$$H_{\rm NM} = \sum_{i=A,B}\left[\sum_{j=g,f,e}\omega_j|j\rangle_{ii}\langle j| + \omega_a a_i^\dagger a_i + (g|e\rangle_{ii}\langle f|a_i + {\rm H.c.})\right] + J(a_A^\dagger a_B + a_A a_B^\dagger), \tag{2}$$

$$H_1 = \frac{\Omega_1}{2}\sum_{i=A,B} {\rm e}^{{\rm i}\omega_1 t}|g\rangle_{ii}\langle e| + {\rm H.c.}, \tag{3}$$

$$H_2 = \frac{\Omega_2}{2}{\rm e}^{{\rm i}\omega_2 t}(|g\rangle_{AA}\langle f| + {\rm e}^{{\rm i}\phi}|g\rangle_{BB}\langle f|) + {\rm H.c.}, \tag{4}$$

where a_i and $a_i^\dagger$ with $i \in \{A,B\}$ represent annihilation and creation operators of the mode of resonator, respectively. ω_1 and ω_2 in the exponentials denote the frequencies of the two microwave fields, respectively. ϕ is the phase difference between two microwave fields for the two superconducting qutrits. J is the photon hopping rate between two transmission line microwave resonators.

Notice that the excitation number operator of the total system $\hat{N} = \sum_{i=A,B}(|e\rangle_{ii}\langle e| + a_i^\dagger a_i)$ is independent of Hamiltonian $H_{\rm NM}$ and H_2, so that the excitation number is conserved under the domination of these two Hamiltonians. Nevertheless, Hamiltonian H_1 would change the excitation number of the system since it does not commute with the excitation number operator. When the Rabi frequency of the first microwave pulse satisfies $\Omega_1 \ll g$ and the system is initially in a state with null excitation, the probability for the system to be excited to the subspace more than a single excitation can be neglected.

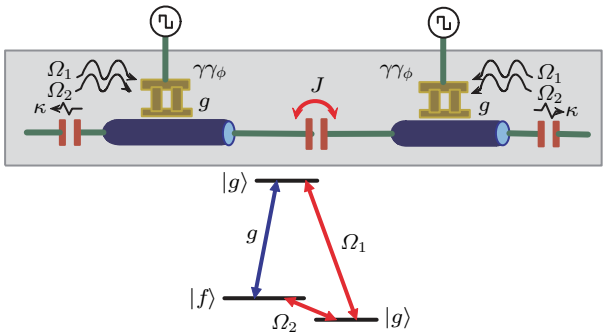


Fig. 1. Experimental schematic illustration for dissipative preparation of entangled steady state between two transmission line microwave resonators coupled through hopping of microwave photons with a hopping rate J in circuit QED. κ, γ, and γ_ϕ are single-photon decay rate, superconducting qutrit spontaneous emission rate, and superconducting qutrit dephasing rate. Each resonator contains a single Λ-type superconducting qutrit which possesses two ground states $|g\rangle$ and $|f\rangle$ and one excited state $|e\rangle$. The qutrit transition $|f\rangle \leftrightarrow |e\rangle$ is resonantly coupled to the resonator with the coupling constant g, and the transitions $|g\rangle \leftrightarrow |e\rangle$ and $|g\rangle \leftrightarrow |f\rangle$ are driven by two microwave fields with Rabi frequencies Ω_1 and Ω_2, respectively.

Here, we obtain the relevant energy eigenstates of Hamiltonian $H_{\rm NM}$ and use them as dressed states within the specific excitation number. The energy of level $|g\rangle$ is taken to be 0 as the energy reference point. In Table 1 and Table 2, we show the eigenstates and the corresponding eigenvalues in zero and single excitation subspaces with the notation

$$|\phi_1\rangle = \frac{1}{V_a}\left(\frac{\sqrt{J^2+g^2}}{g}|fg,10\rangle + \frac{J}{g}|fg,01\rangle + |eg,00\rangle\right),$$

$$|\phi_2\rangle = \frac{1}{V_a}\left(\frac{J}{g}|gf,10\rangle + \frac{\sqrt{J^2+g^2}}{g}|gf,01\rangle + |ge,00\rangle\right),$$

$$|\phi_3\rangle = \frac{1}{V_a}\left(\frac{J}{g}|fg,01\rangle - \frac{\sqrt{J^2+g^2}}{g}|fg,10\rangle + |eg,00\rangle\right),$$

$$|\phi_4\rangle = \frac{1}{V_a}\left(\frac{J}{g}|gf,10\rangle - \frac{\sqrt{J^2+g^2}}{g}|gf,01\rangle + |ge,00\rangle\right),$$

$$|\phi_5\rangle = \frac{1}{V_b}\left(-\frac{J}{g}|fg,01\rangle + |eg,00\rangle\right),$$

$$|\phi_6\rangle = \frac{1}{V_b}\left(-\frac{J}{g}|gf,10\rangle + |ge,00\rangle\right),$$

$$|\phi_7\rangle = \frac{1}{\sqrt{2}}(|gg,10\rangle - |gg,01\rangle),$$

$$|\phi_8\rangle = \frac{1}{\sqrt{2}}(|gg,10\rangle + |gg,01\rangle),$$

$$|\phi_9\rangle = \frac{1}{V_d}\left[\frac{J-\sqrt{J^2+4g^2}}{2g}(|ff,10\rangle - |ff,01\rangle) - |ef,00\rangle + |fe,00\rangle\right],$$

$$|\phi_{10}\rangle = \frac{1}{V_e}\left[\frac{J+\sqrt{J^2+4g^2}}{2g}(|ff,10\rangle - |ff,01\rangle) - |ef,00\rangle + |fe,00\rangle\right],$$

$$|\phi_{11}\rangle = \frac{1}{V_d}\left[\frac{J-\sqrt{J^2+4g^2}}{2g}(|ff,10\rangle + |ff,01\rangle) + |ef,00\rangle\right.$$

$$+|fe,00\rangle\Big],$$
$$|\phi_{12}\rangle=\frac{1}{V_e}\Big[\frac{J+\sqrt{J^2+4g^2}}{2g}(|ff,10\rangle+|ff,01\rangle)+|ef,00\rangle+|fe,00\rangle\Big], \quad (5)$$

with

$$V_a=\sqrt{2(J^2/g^2+1)},\quad V_b=\sqrt{(J^2/g^2+1)},$$
$$V_d=\sqrt{J^2/g^2+4-J\sqrt{J^2+4g^2}/g^2},$$
$$V_e=\sqrt{J^2/g^2+4+J\sqrt{J^2+4g^2}/g^2}.$$

Table 1. The eigenstates and eigenenergies of the Hamiltonian $H_{\rm NM}$ within the null-excitation subspace. Here the notation $|AB,CD\rangle$ represents that atom 1 (2) is in the state $|A\rangle$ ($|B\rangle$) and there are $C(D)$ photons in cavity 1 (2).

Eigenstate	Eigenenergy
$\|gg,00\rangle$	0
$\|T,00\rangle=1/\sqrt{2}(\|gf,00\rangle+\|fg,00\rangle)$	ω_f
$\|S,00\rangle=1/\sqrt{2}(\|gf,00\rangle-\|fg,00\rangle)$	ω_f
$\|ff,00\rangle$	$2\omega_f$

Table 2. The eigenstates and eigenenergies of the Hamiltonian $H_{\rm NM}$ within the single-excitation subspace.

Eigenstate	Eigenenergy
$\|\phi_1\rangle$,$\|\phi_2\rangle$	$\lambda_1=\lambda_2=\omega_e+\sqrt{J^2+g^2}$
$\|\phi_3\rangle$,$\|\phi_4\rangle$	$\lambda_3=\lambda_4=\omega_e-\sqrt{J^2+g^2}$
$\|\phi_5\rangle$,$\|\phi_6\rangle$	$\lambda_5=\lambda_6=\omega_e$
$\|\phi_7\rangle$	$\lambda_7=\omega_e-\omega_f-J$
$\|\phi_8\rangle$	$\lambda_8=\omega_e-\omega_f+J$
$\|\phi_9\rangle$	$\lambda_9=\omega_f+\omega_e-J/2+\sqrt{J^2+4g^2}/2$
$\|\phi_{10}\rangle$	$\lambda_{10}=\omega_f+\omega_e-J/2-\sqrt{J^2+4g^2}/2$
$\|\phi_{11}\rangle$	$\lambda_{11}=\omega_f+\omega_e+J/2-\sqrt{J^2+4g^2}/2$
$\|\phi_{12}\rangle$	$\lambda_{12}=\omega_f+\omega_e+J/2+\sqrt{J^2+4g^2}/2$

The different energy gaps between these dressed states provide the possibility to drive the specific transitions of the system with extra microwave fields.

3. Engineering steady-state entanglement of two transmons by dissipation dynamics with microwave pulses

We let the second microwave pulses applied to two transmons to be opposite in phase, *i.e.*, $\phi=\pi$ in the Hamiltonian H_2. In order to see clearly the roles of H_1 and H_2, we reexpress them in the dressed state subspace and move to the interaction picture with respect to the Hamiltonian $H_{\rm NM}$. Then the Hamiltonian H_1 can be rewritten as

$$H_1=\frac{\Omega_1}{2V_a}\sum_{k=1}^{6}\mathrm{e}^{\mathrm{i}(\omega_1-\lambda_k)t}|gg,00\rangle\langle\phi_k|-\frac{\Omega_1}{\sqrt{2}}\frac{1}{V_d}\mathrm{e}^{\mathrm{i}(\omega_1+\omega_f-\lambda_9)t}|S,00\rangle\langle\phi_9|+\frac{\Omega_1}{\sqrt{2}}\frac{1}{V_d}\mathrm{e}^{\mathrm{i}(\omega_1+\omega_f-\lambda_{11})t}|T,00\rangle\langle\phi_{11}|-\frac{\Omega_1}{\sqrt{2}}\frac{1}{V_e}\mathrm{e}^{\mathrm{i}(\omega_1+\omega_f-\lambda_{10})t}|S,00\rangle\langle\phi_{10}|+\frac{\Omega_1}{\sqrt{2}}\frac{1}{V_e}\mathrm{e}^{\mathrm{i}(\omega_1+\omega_f-\lambda_{12})t}|T,00\rangle\langle\phi_{12}|+\mathrm{H.c.} \quad (6)$$

Similarly, H_2 can be rewritten as

$$H_2=\frac{1}{\sqrt{2}}\Omega_2(|S,00\rangle\langle 00,ff|-|gg,00\rangle\langle 00,S|)+\mathrm{H.c.} \quad (7)$$

Equation (6) indicates the transition between the states in zero excitation subspace and one excitation subspace. From Eq. (7), one can see that microwave field Ω_2 leads to the resonant transitions among the states $|ff,00\rangle$, $|S,00\rangle$, and $|gg,00\rangle$.

The dynamics of open dissipative system in Lindblad form is described by the master equation

$$\dot{\hat{\rho}}=\mathrm{i}[\hat{\rho},H]+\frac{1}{2}\sum_j\left[2\hat{\mathcal{L}}_j\hat{\rho}\hat{\mathcal{L}}_j^\dagger-(\hat{\mathcal{L}}_j^\dagger\hat{\mathcal{L}}_j\hat{\rho}+\hat{\rho}\hat{\mathcal{L}}_j^\dagger\hat{\mathcal{L}}_j)\right], \quad (8)$$

where $\hat{\mathcal{L}}_j$ is the so-called Lindblad operators governing dissipation. Specifically, in the current scheme the Lindblad operators can be expressed as

$$\hat{\mathcal{L}}_{\gamma 1}=\sqrt{\gamma/2}|g\rangle_{AA}\langle e|,\quad \hat{\mathcal{L}}_{\gamma 2}=\sqrt{\gamma/2}|f\rangle_{AA}\langle e|,$$
$$\hat{\mathcal{L}}_{\gamma 3}=\sqrt{\gamma/2}|g\rangle_{BB}\langle e|,\quad \hat{\mathcal{L}}_{\gamma 4}=\sqrt{\gamma/2}|f\rangle_{BB}\langle e|,$$
$$\hat{\mathcal{L}}_{\kappa 1}=\sqrt{\kappa}a_A,\quad \hat{\mathcal{L}}_{\kappa 2}=\sqrt{\kappa}a_B,$$
$$\hat{\mathcal{L}}_{\gamma_{\phi 1}}=\sqrt{\gamma_\phi/2}(|e\rangle_{AA}\langle e|-|g\rangle_{AA}\langle g|),$$
$$\hat{\mathcal{L}}_{\gamma_{\phi 2}}=\sqrt{\gamma_\phi/2}(|e\rangle_{AA}\langle e|-|f\rangle_{AA}\langle f|),$$
$$\hat{\mathcal{L}}_{\gamma_{\phi 3}}=\sqrt{\gamma_\phi/2}(|e\rangle_{BB}\langle e|-|g\rangle_{BB}\langle g|),$$
$$\hat{\mathcal{L}}_{\gamma_{\phi 4}}=\sqrt{\gamma_\phi/2}(|e\rangle_{BB}\langle e|-|f\rangle_{BB}\langle f|),$$

$\hat{\mathcal{L}}_{\gamma 1(3)}$ and $\hat{\mathcal{L}}_{\gamma 2(4)}$ describe the dissipation induced by the qutrit decay, $\hat{\mathcal{L}}_{\kappa 1(2)}=\sqrt{\kappa}a_{A(B)}$ is the dissipation induced by the single photon decay of resonator $A(B)$, $\hat{\mathcal{L}}_{\gamma_{\phi 1(3)}}$ and $\hat{\mathcal{L}}_{\gamma_{\phi 2(4)}}$ are the dissipations induced by the qutrit dephasing.

The processes for producing and stabilizing the Bell state $|T,00\rangle$ is shown in Fig. 2 which presents four preparation channels. By choosing different frequency ω_1 of the first microwave field, the target state can be prepared in different ways. This is due to the fact that the microwave field Ω_1 with specified frequency can drive a certain resonant couplings between the states in zero subspace and one excitation subspace, but the transitions from $|T,00\rangle$ to the states in the one excitation subspace are non-resonant. In Fig. 2(a), by choosing ω_1=$\omega_e-\sqrt{J^2+g^2}$, the state $|gg,00\rangle$ would couple resonantly to $|\phi_3\rangle$ and $|\phi_4\rangle$ while the other terms in Eq. (5) undergo non-resonant transitions with different detunings. Affected by the dissipative factors mentioned in Eq. (8), the $|\phi_3\rangle$ and $|\phi_4\rangle$ would be converted to $|fg,00\rangle$ and $|gf,00\rangle$,

which is a superposition of the states $|T,00\rangle$ and $|S,00\rangle$. As has been shown that the state $|S,00\rangle$ can be driven to ground state $|gg,00\rangle$ by microwave field Ω_2, which would be redriven to the states $|\phi_3\rangle$ and $|\phi_4\rangle$, while the state $|T,00\rangle$ is far off-resonant with microwave field Ω_1. This means that the population of $|T,00\rangle$ will accumulate with time increasing. Similarly, this target state $|T,00\rangle$ also can be achieved through the other three channels in Figs. 2(b)–2(d) by choosing $\omega_1 = \omega_e$, $\omega_e + \sqrt{J^2+4g^2}/2 - J/2$, and $\omega_e - \sqrt{J^2+4g^2}/2 - J/2$, respectively.

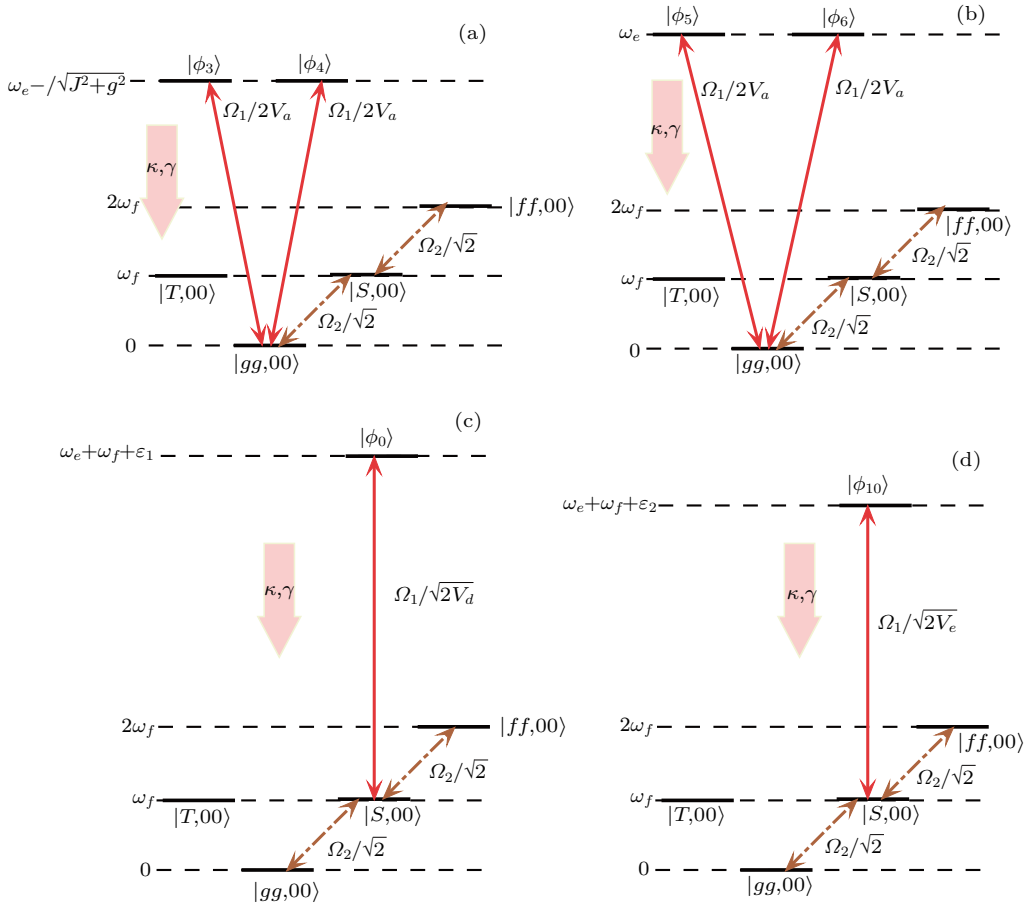


Fig. 2. Level configuration and transitions in the dressed state picture, the microwave field Ω_2 causes resonant transitions among states $|gg,00\rangle$, $|S,00\rangle$, and $|ff,00\rangle$ in null excitation subspace by choosing the frequency suitably, while microwave field Ω_1 causes resonant transitions forming the following four preparation channels: (a) $|gg,00\rangle \Leftrightarrow \{|\phi_3\rangle, |\phi_4\rangle\}$ with $\omega_1 = \omega_e - \sqrt{J^2+g^2}$, (b) $|gg,00\rangle \Leftrightarrow \{|\phi_5\rangle, |\phi_6\rangle\}$ with $\omega_1 = \omega_e$, (c) $|S,00\rangle \Leftrightarrow |\phi_9\rangle$ with $\omega_1 = \omega_e + \sqrt{J^2+4g^2}/2 - J/2$, and (d) $|S,00\rangle \Leftrightarrow |\phi_{10}\rangle$ with $\omega_1 = \omega_e - \sqrt{J^2+4g^2}/2 - J/2$, respectively, but the transitions from $|T,00\rangle$ to the states in the one excitation subspace is non-resonant. The notations ξ_1 and ξ_2 in the figure are defined as ξ_1=$\sqrt{J^2+4g^2}$/2-J/2 and ξ_2=-$\sqrt{J^2+4g^2}$/2-J/2.

4. Numerical simulation

To demonstrate the feasibility of our Bell-state stabilization mechanism, we assess the performance of our scheme by numerically solving the Lindblad master equation. In Fig. 3, we plot the fidelity of the states in null excitation with optimized parameters corresponding to the four preparation channels in Fig. 2. The results show that the target state could be prepared for different choice of the ω_1 with fidelity 91.28%, 97.09%, 93.15%, and 87.93%, respectively. In addition, in order to verify the quantum coherence degree of the target state, we also consider the Clauser–Horne–Shimony–Holt (CHSH) correlation $S(t)$ which is defined as

$$S(t) = \mathrm{Tr}\left[(\mathcal{O}_{\mathrm{CHSH}})\rho(t)\right] \tag{9}$$

with

$$\mathcal{O}_{\mathrm{CHSH}} = \sigma_{y,1} \otimes \frac{-\sigma_{y,2} - \sigma_{x,2}}{\sqrt{2}} + \sigma_{x,1} \otimes \frac{-\sigma_{y,2} - \sigma_{x,2}}{\sqrt{2}} + \sigma_{x,1} \otimes \frac{\sigma_{y,2} - \sigma_{x,2}}{\sqrt{2}} - \sigma_{y,1} \otimes \frac{\sigma_{y,2} - \sigma_{x,2}}{\sqrt{2}}, \tag{10}$$

where $\sigma_{x,1}(\sigma_{x,2})$ and $\sigma_{y,1}(\sigma_{y,2})$ being Pauli operators of the superconducting qutrit. With the achievable experimental parameters[44] $\Omega_1 = \Omega_2 = 0.0275g$, $\kappa = 0.035g$, $\gamma = (1/3600)g$, and $\gamma_\phi = (1/14400)g$, and setting $\omega_1 = \omega_e$, the CHSH correlation is plotted in Fig. 4. It can be seen that the CHSH correlation reaches about 2.714, obviously exceeding the maximum value 2 allowed by the local hidden variable theories. Besides, to verify the robustness of the scheme for the driving amplitudes, we plot the fidelity of the target steady-state as a function of the Rabi frequencies Ω_1 and Ω_2 for given

parameters κ, γ, and γ_ϕ in Fig. 5(a), the results show that a fidelity higher than 90% can be achieved for a wide range of Rabi frequencies, demonstrating the scheme is insensitive to deviations of these control parameters. In Fig. 5(b), we consider the two dissipative factors at the same time and plot the variance of the fidelity of the target state. It shows that the fidelity increases steeply with the increasing in κ and γ, and the

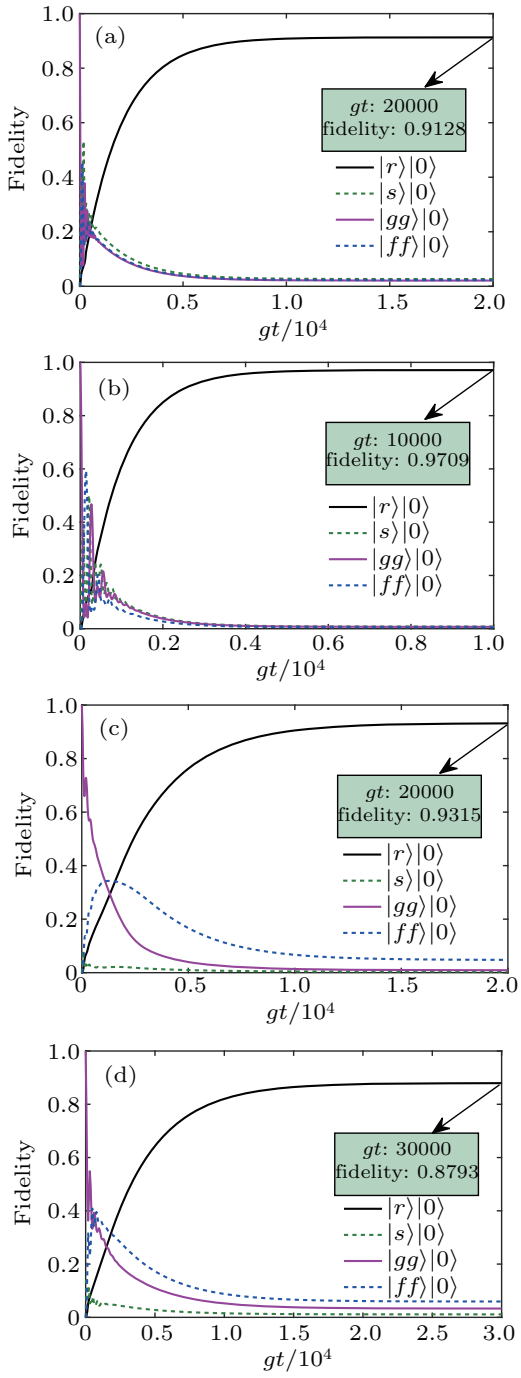


Fig. 3. Populations of $|T,00\rangle$, $|S,00\rangle$, $|gg,00\rangle$, $|ff,00\rangle$ corresponding to four channels in Fig. 2 with the initial state $|gg,00\rangle$. The optimized parameters are chosen as (a) $\Omega_1 = 0.066g$, $\Omega_2 = 0.02g$, $J = 1.2g$, $\kappa = \gamma = 0.022g$, $\gamma_\phi = 6.8\times10^{-5}g$, and $\omega_1 = \omega_e - \sqrt{J^2+g^2}$. (b) $\Omega_1 = 0.026g$, $\Omega_2 = 0.02g$, $J = 1.1g$, $\kappa = \gamma = 0.01g$, $\gamma_\phi = 6.8\times10^{-5}g$, and $\omega_1 = \omega_e$. (c) $\Omega_1 = 0.065g$, $\Omega_2 = 0.012g$, $J = 1.5g$, $\kappa = 0.008g$, $\gamma = 0.01g$, $\gamma_\phi = 6.8\times10^{-5}g$, and $\omega_1 = \omega_e + \sqrt{J^2+4g^2}/2 - J/2$. (d) $\Omega_1 = 0.063g$, $\Omega_2 = 0.012g$, $J = 0.8g$, $\kappa = 0.0008g$, $\gamma = 0.012g$, $\gamma_\phi = 6.8\times10^{-5}g$, and $\omega_1 = \omega_e - \sqrt{J^2+4g^2}/2 - J/2$.

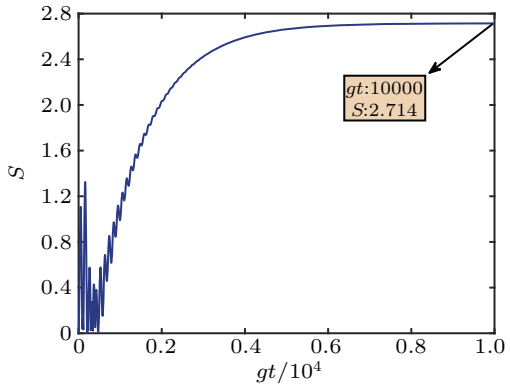


Fig. 4. The CHSH correlation of the target steady state as a function of the time. We choose the experimental parameters: $\Omega_1 = \Omega_2 = 0.0275g$, $J = 1.1g$, $\kappa = 0.035g$, $\gamma = (1/3600)g$, and $\gamma_\phi = (1/14400)g$.

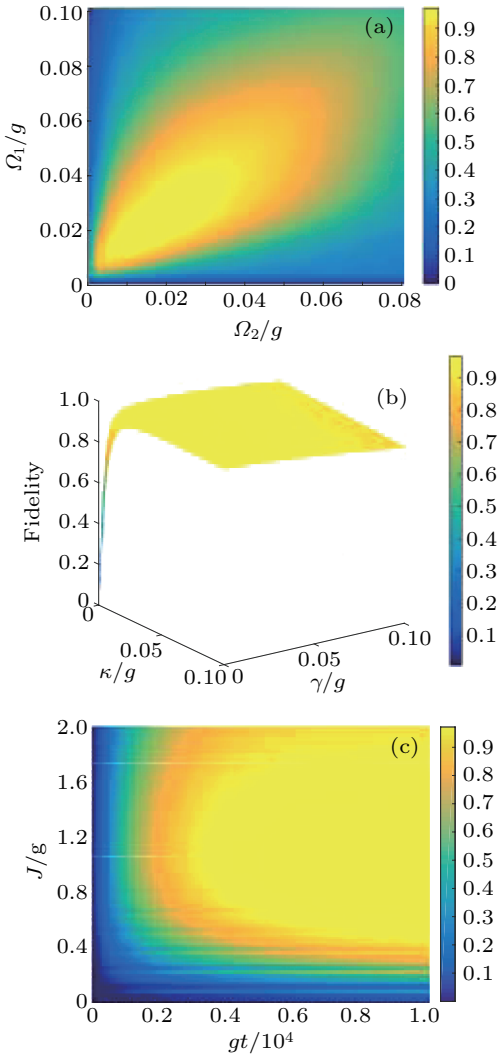


Fig. 5. (a) The fidelity of the target steady state as a function of the Rabi frequencies Ω_1 and Ω_2 with the initial state $|gg,00\rangle$ at time $1\times10^4/g$. (b) The fidelity of the target steady state *versus* the variance of the single-photon decay κ and qubit decay γ at time $1\times10^4/g$. (c) The fidelity of the target steady state *versus* photon hopping rate J and evolution time. The rest of the parameters are the same as those in Fig. 4.

optimal fidelity is about 96.73%. However, further increase in the dissipative factors would reduce the performance of the scheme. In Fig. 5(c), the fidelity *versus* J and evolution time shows that the robustness of the scheme against the variations

of the coupling strength between two transmission line microwave resonators, in which the fidelity can reach 90% even when the parameter is taken as $J = 0.45g$.

Since charge noise may causes random fluctuations of the qutrit frequency in circuit QED, resulting in dephasing,[45] different from the qutrit decay and photon decay of the resonator, qutrit dephasing is a detrimental effect for the current scheme. In Fig. 6, the influence of dephasing is considered and the fidelity of the target state is plotted when the system is in stabilization (for the evolution time $t = 1 \times 10^4/g$). The fidelity can be observed to monotonously increase with κ/γ_ϕ. The fidelity can be higher than 90% when the ratio appears about $\kappa/\gamma_\phi \geq 960$. This result occurs because qutrit dephasing results in a population transfer between the singlet states $|T\rangle$ and $|S\rangle$, decreasing the fidelity of the target steady-state.

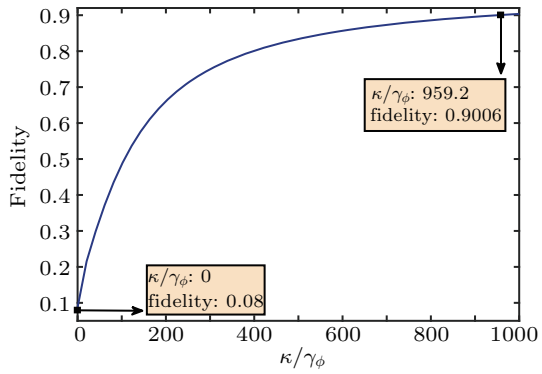


Fig. 6. The fidelity of the target steady-state, plotted *versus* different ratios κ/γ_ϕ. The rest of the parameters are the same as those in Fig. 4.

5. Conclusion

In conclusion, we have proposed a dissipative scheme for creating an entangled steady-state between two transmons separately interacts with two coupled transmission line resonators in circuit QED. The combination of coherent driving fields and dissipative processes would drive the system into a steady-state. By choosing different frequencies of the microwave field, the target steady-state can be generated with different preparation channels. The numerical simulations and analysis show that the present scheme is robust against the qutrit decay and the cavity decay due to they are used as the positive resources in the scheme. Since the transmon qubits have been demonstrated in experiments as well as its scalability in circuit QED, the current scheme can be used to physical realization of quantum computer and quantum communication.

Acknowledgment

This work was supported by the Yanbian University Hospital.

References

[1] Einstein A, Podolsky B and Rosen N 1935 *Phys. Rev. A* **47** 777
[2] Schrödinger E 1935 *Naturwissenschaften* **23** 823
[3] Horodechi R, Horodeck P, Horodecki M and Horodecki K 2009 *Rev. Mod. Phys.* **81** 865
[4] Lee K C, Sprague M R, Sussman B J, Nunn J, Langford N K, Jin X M, Champion T, Michelberger P, Reim K F, England D, Jaksch D and Walmsley I A 2011 *Science* **334** 1253
[5] Vacanti G and Beige A 2009 *New J. Phys.* **11** 083008
[6] Lin Y, Gaebler J P, Reiter F, Tan T R, Bowler R, Sørensen R S, Leibfried D and Wineland D J 2013 *Nature* **504** 415
[7] Carr A W and Saffman M 2013 *Phys. Rev. Lett.* **111** 033607
[8] Man Z X, Xia Y J, and Franco R L 2015 *Sci. Rep.* **8** 13843
[9] Plenio M B, Huelga S F, Beige A and Knigh P L 1999 *Phys. Rev. A* **59** 2468
[10] Clark S, Peng A, Gu M and Parkins S 2003 *Phys. Rev. Lett.* **91** 177901
[11] Busch J, De S, Ivanov S S, Torosov B T, Spiller T P and Beige A 2011 *Phys. Rev. A* **84** 022316
[12] Kastoryano M J, Reiter F and Sørensen A S 2011 *Phys. Rev. Lett.* **106** 090502
[13] Reiter F, Kastoryano M J and Sørensen A S 2012 *New J. Phys.* **14** 053022
[14] Shen L T, Chen X Y, Yang Z B, Wu H Z and Zheng S B 2011 *Phys. Rev. A* **84** 064302
[15] Shen L T, Chen X Y, Yang Z B, Wu H Z and Zheng S B 2012 *Europhys. Lett.* **99** 20003
[16] Shen L T, Chen X Y, Yang Z B, Wu H Z and Zheng S B 2013 *Quantum Inf. Comput.* **13** 281
[17] Shen L T, Chen X Y, Yang Z B, Wu H Z and Zheng S B 2014 *Opt. Lett.* **39** 6046
[18] Su S L, Shao X Q, Wang H F and Zhang S 2014 *Phys. Rev. A* **90** 054302
[19] Su S L, Shao X Q, Wang H F and Zhang S 2014 *Sci. Rep.* **4** 7566
[20] Su S L, Guo Q, Wang H F and Zhang S 2015 *Phys. Rev. A* **92** 022328
[21] Su S L, Shao X Q, Guo Q, Cheng L Y, Wang H F and Zhang S 2015 *Eur. Phys. J. D* **69** 123
[22] Zheng S B and Shen L T 2014 *J. Phys. B: At. Mol. Opt. Phys.* **47** 055502
[23] Shao X Q, You J B, Zheng T Y, Oh C H and Zhang S 2014 *Phys. Rev. A* **89** 012319
[24] Shao X Q, You J B, Zheng T Y, Oh C H and Zhang S 2014 *Phys. Rev. A* **89** 052313
[25] Parkins A S, Solano E and Cirac J I 2006 *Phys. Rev. Lett.* **96** 053602
[26] Muschik C A, Polzik E S and Cirac J I 2011 *Phys. Rev. A* **83** 052312
[27] Dalla Torre E G, Otterbach J, Demler E, Vuletic V and Lukin M D 2013 *Phys. Rev. Lett.* **110** 120402
[28] Poyatos J F, Cirac J I and Zoller P 1996 *Phys. Rev. Lett.* **77** 4728
[29] Cho J, Bose S and Kim M S 2011 *Phys. Rev. Lett.* **106** 020504
[30] Barreiro J T, Muller M, Schindler P, Nigg D, Monz T, Chwalla M, Hennrich M, Roos C F, Zoller P and Blatt R 2011 *Nature* **470** 486
[31] Gonzalez-Tudela A, Martín-Cano D, Moreno E, MartínMoreno L, Tejedor C and García-Vidal F J 2011 *Phys. Rev. Lett.* **106** 020501
[32] Gullans M, Tiecke T G, Chang D E, Feist J, Thompson J D, Cirac J I, Zoller P and Lukin M D 2012 *Phys. Rev. Lett.* **109** 235309
[33] Gonzalez-Tudela A and Porras D 2013 *Phys. Rev. Lett.* **110** 080502
[34] Diehl S, Micheli A, Kantian A, Kraus B, Büchler H P and Zoller P 2008 *Nat. Phys.* **4** 878
[35] Foss-Feig M, Daley A J, Thompson J K and Rey A M 2012 *Phys. Rev. Lett.* **109** 230501
[36] Krauter H, Muschik C A, Jensen K, Wasilewski W, Petersen J M, Cirac J I and Polzik E S 2011 *Phys. Rev. Lett.* **107** 080503
[37] Schmidt S, Houck A A, Blatter G and Türeci H E 2010 *Phys. Rev. B* **82** 100507(R)
[38] Clarke J and Wilhelm F K 2008 *Nature* **453** 1031
[39] Makiilin Y, Schon G and Siinirman A 2001 *Rev. Mod. Phys.* **73** 357
[40] Wendin G and Shumeikoa V S 2007 *Low Temp. Phys.* **33** 724
[41] Yu Y, Han S, Chu X, Chu S I and Wang Z 2002 *Science* **296** 889
[42] Raftery J, Sadri D, Schmidt S, Treci H E and Houck A A 2014 *Phys. Rev. X* **4** 031043
[43] Wallraff A, Schuster D I, Blais A, Frunzio L, Huang R S, Majer J, Kumar S, Girvin S M and Schoelkopf R J 2004 *Nature* **431** 162-167
[44] Shankar S, Hatridge M, Leghtas Z, Sliwa K M, Narla A, Vool U, Girvin S M, Frunzio L, Mirrahimi M and Devoret M H 2013 *Nature* **504** 419
[45] Schreier J A, Houck A A, Koch J, Schuster D I, Johnson B R, Chow J M, Gambetta J M, Majer J, Frunzio L, Devoret M H, Girvin S M and Schoelkopf R J 2008 *Phys. Rev. B* **77** 180502(R)